

# Specific Solvent Effects of Hydroxylic Solvents on the Emission Properties of Ruthenium(II)tris(2,2'-bipyridyl) Chloride

P. Hartmann,<sup>1,2</sup> M. J. P. Leiner,<sup>1,3</sup> and M. E. Lippitsch<sup>2</sup>

---

The excited state of Ru(II)[bpy]<sub>3</sub><sup>2+</sup> dissolved in hydroxylic solvents is subject to specific solvent effects, which were hitherto not understood on a quantitative basis. We determined the solvent effects of linear monovalent alcohols on the energy gap law of internal conversion with the help of lifetime and intensity measurements. An on-line method for measurement of the temperature dependence of quantum efficiencies was introduced. A modified Franck-Condon analysis of emission spectra by taking into account the shape of a Morse potential of the involved states was applied to compute excited-state energies.

---

**KEY WORDS:** Ru(II) complexes; energy gap law; alcohols.

## INTRODUCTION

The photophysical and photochemical behavior of Ru(II)[bpy]<sub>3</sub><sup>2+4</sup> and related molecules in solution is well established [1]. Nonradiative decay can be described in terms of the energy gap law [2], which predicts a linear dependence of the natural logarithm of the nonradiative decay rate  $\ln(k_{nr})$  of the excited MLCT state on the energy difference  $E_{00}$  between the zero-point vibrational levels of ground and excited states:  $\ln(k_{nr})$  decreases with increasing  $E_{00}$ .

Hydroxylic solvents provide specific interactions (via hydrogen bonds) with the indicator, which lead to deviations of the overall nonradiative decay rate from the behavior expected for nonhydroxylic solvents [2b,3].

We systematically investigated the nonradiative decay properties of Ru(II)[bpy]<sub>3</sub><sup>2+</sup> dissolved in linear monovalent alcohols up to 1-decanol, with the help of

absorption spectroscopy and intensity- as well as lifetime-based fluorescence spectroscopy. The problem was complicated by the fact that low-lying d-d states of the molecule give rise to thermally activated nonradiative decay [4] and photochemistry [2b].

However, we were able to separate the measured overall nonradiative decay rate  $k_{nr}$  into contributions of

- (1) thermal activation of the d-d states ( $k_{nr,dd}$ );
- (2) deactivation via the energy gap ( $k_{nr,eg}$ ); and
- (3) a specific rate,  $k_{nr,OH}$ , induced by effects of the hydroxylic environment of the molecule.

$$k_{nr} = k_{nr,dd} + k_{nr,eg} + k_{nr,OH} \quad (1a)$$

We also introduce the temperature-independent nonradiative decay rate  $k_{nr,o}$ :

$$k_{nr,o} = k_{nr} - k_{nr,dd} \quad (1b)$$

<sup>1</sup> AVL List GmbH, Biomedical Research and Development, Kleists-  
traÙe 48, A-8020 Graz, Austria.

<sup>2</sup> Institut für Experimentalphysik, Karl-Franzens-Universität, Univer-  
sitätspl. 5, A-8010 Graz, Austria.

<sup>3</sup> To whom correspondence should be addressed.

<sup>4</sup> Abbreviations used: Ru(II)[bpy]<sub>3</sub><sup>2+</sup>, ruthenium(II)tris(2,2'-bipyridyl)  
chloride; MLCT, metal-to-ligand charge transfer; PMT, photomulti-  
plier tube.

## EXPERIMENTAL

Emission spectra (corrected for solvent background and PMT response) and quantum efficiencies were determined at  $25 \pm 1^\circ\text{C}$  with a SPEX Fluorolog II spectrofluorimeter, equipped with a 450-W xenon-arc lamp and a Hamamatsu R 928 PMT. Lifetime measurements were performed at  $25 \pm 1^\circ\text{C}$  with a PRA LN102 dye laser, pumped by a PRA LN103 nitrogen laser (excitation at  $\lambda = 470$  nm). Emission was monitored through a Schott KV550 cutoff filter, a VALVO TUVF 56 PMT, and a 1-GHz Tektronix DSA601A digital signal analyzer.  $\text{Ru(II)[bpy]}_3^{2+}(\text{Cl}^-)_2$  was used as received from Strem chemicals. Solvents were at least reaction grade and used without further purification. Quantum efficiencies at room temperature were determined by a modified Parker-Rees method [5]. Temperature dependence of quantum efficiencies was determined by illuminating the solution in a thermostated chamber in the fluorimeter (wavelength  $\lambda = 470$  nm). The sample was heated to approximately  $60^\circ\text{C}$  (dependent on the solvent boiling point). By slowly cooling down to room temperature (quasi-steady-state measurement), intensity was simultaneously monitored at the wavelength of  $\lambda = 610$  nm. Quantum efficiencies at  $25^\circ\text{C}$  were used to calibrate the temperature curve of the intensity signal.

Evaluation of quantum efficiencies is more inaccurate compared to lifetime measurements, which are commonly used for the determination of the temperature dependence of photophysical parameters [4]. However, with the chosen on-line method, this disadvantage is overcompensated by a high number of recorded temperature values ( $n = 360$ ). Additionally, data treatment after the measurement is easier, since lifetime measurements would additionally require fits of the recorded decay curves at each temperature.

After calibration the obtained temperature curve of quantum efficiency  $\Phi(T)$  was fitted to the established equation (2):

$$\Phi(T) = \frac{k_r}{k_o + k' \exp(-E_a / kT)} \quad (2)$$

$k_r$  is the radiative decay rate,  $k_o$  the temperature-independent part of the overall radiative and nonradiative decay rates,  $k'$  the frequency of the thermal activated decay via d-d-states,  $E_a$  the activation energy, and  $k$  the Boltzmann constant.

The emission energy  $E_{oo}$  was calculated by a Franck-Condon analysis [2b,6] of the corrected emission spectra  $I(E)$ , modified by introducing a Morse

potential [7] to obtain a better approach to the real distribution of energy levels.

$$I(E) = \sum_{\nu=0}^4 \left[ \left( \frac{E_{oo} - h\nu_m (\nu - (\nu^2 + \nu) \cdot x_e)}{E_{oo}} \right)^4 \cdot \frac{S_m^\nu}{\nu!} \cdot \exp \left( -4 \ln(2) \cdot \left( \frac{E - E_{oo} + h\nu_m (\nu - (\nu^2 + \nu) \cdot x_e)}{h\nu_{1/2}} \right)^2 \right) \right] \quad (3)$$

$E_{oo}$  is the energy difference between the zero point vibrational levels of excited state and ground state,  $h\nu_m$  the effective energy of the high-frequency vibrations responsible for deactivation of the excited state,  $\nu$  the vibrational quantum number of the ground-state framework stretching vibrations of the ligands which significantly contribute to the observed emission spectra [8],  $S_m$  the dimensionless fractional displacement of the effective normal mode between the equilibrium configurations of the ground and excited states,  $\nu_{1/2}$  the full width at half-maximum of an individual vibrational component, and  $x_e$  the anharmonicity parameter of the Morse potential.

## RESULTS AND DISCUSSION

For an indicator dissolved in various homogeneous one-component solvents, the plot of  $\ln(k')$  versus  $E_a$  gives a straight line with  $1/kT$  as the slope (Barclay-Butler plot) [9]. A linear regression of the data to Eq. (4) is employed instead of the more inaccurate original data of  $k'$  and  $E_a$  to evaluate the thermal activated decay rate  $k_{nr,dd}$ .

$$\ln(k_{nr,dd}) = \ln(k') - E_a/kT \quad (4)$$

The linear regression parameters obtained are

$$\begin{aligned} \ln(k_{nr,dd}) &= 12.97 \\ 1/kT &= 4.89 \cdot 10^{-3} \text{ cm} \end{aligned}$$

After subtraction of the temperature-induced decay via d-d states ( $k_{nr,dd}$ ) from the overall decay rate  $k_{nr}$  [10], the energy gap law behavior becomes apparent (Fig. 2). In contrast to the behavior of  $\text{Ru(II)[bpy]}_3^{2+}$  in nonhydroxylic solvents [2b], where the logarithm of the remaining rate  $k_{nr,o}$  decreases linearly with increasing excited-state energy (dashed line in Fig. 2), an increase in  $\ln(k_{nr,o})$  is observed. By comparison with the behavior of  $\ln(k_{nr,o})$  in nonhydroxylic solvents, one obtains directly the rate

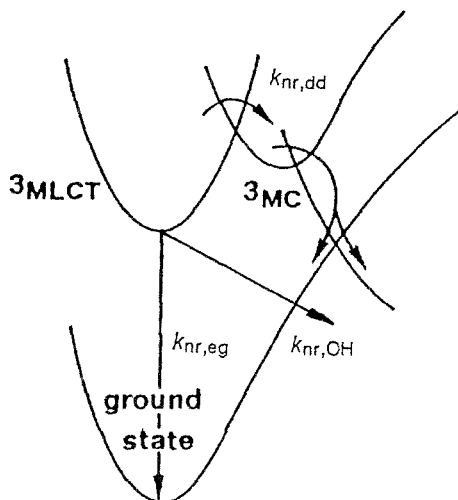


Fig. 1. Schematic representation of the potential curves and pathways involved in nonradiative decay.

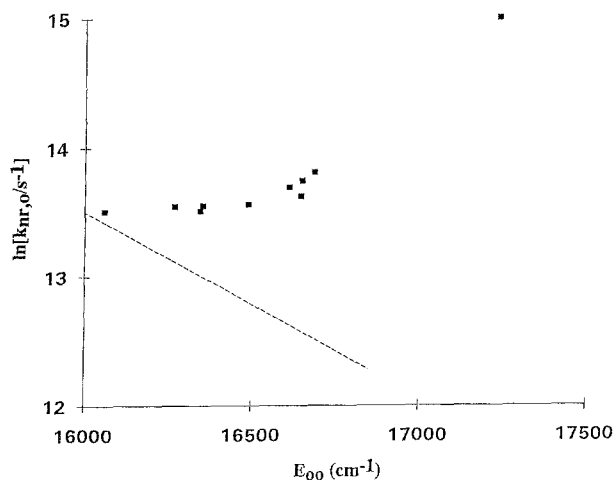


Fig. 2. Logarithmic representation of the temperature-independent part of the nonradiative decay rate  $k_{nr,o}$  as a function of excited-state energy  $E_{oo}$ . The energy gap law of nonhydroxylic solvents (dashed line) is taken from Ref. 2b.

of nonradiative decay induced by the hydroxylic solvents as  $\ln(k_{nr,OH})$ .

As a result a plot of  $\ln(k_{nr,OH})$  versus  $E_{oo}$  yields a straight line for the indicator dissolved in linear monovalent alcohols, including trifluoroethanol (Fig. 3).  $\ln(k_{nr,OH})$  is higher for the more polar solvents (methanol, ethanol, propanol, and especially trifluoroethanol) and lower for the apolar long-chain alcohols.

The origin of the effect can therefore be attributed to the interaction of the polar OH groups of the solvent molecules, which is assumed to proceed via H bonds

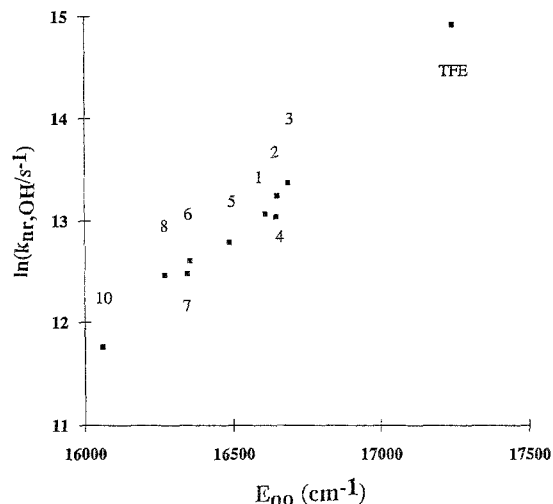


Fig. 3. Logarithmic representation of the specific rate  $k_{nr,OH}$ , induced by effects of the hydroxylic environment as a function of excited-state energy  $E_{oo}$ . The insets indicate the numbers of C atoms of the respective linear monovalent alcohols. TFE is 2,2,2-trifluoroethanol.

and dipole forces between the Ru(II)-ion and the solvent molecule. This is confirmed by considering the effect of 2,2,2-trifluoroethanol (Fig. 3) (three F atoms replacing three H atoms of ethanol), which has the highest influence on the decay rate.

In the case of the long-chain alcohols, however, the apolar tail of C atoms dominates the solvent effects and therefore the influence of the OH groups is suppressed.

The results of this behavior can be enumerated as a distortion energy term within energy gap law theory. The obtained values [10] for this term are not negligible compared to those of  $E_{oo}$ , indicating a strong influence of the solvent.

High-frequency vibrations of the solvent molecules are supposed to act as the promoting modes for the enhanced radiationless deactivation of the excited state of Ru(II)[bpy]<sub>3</sub><sup>2+</sup> in hydroxylic solvents [2b,9]. From microwave absorption measurements [11] the nature of those vibrations is attributed to rotations of the OH group around the C–O axis.

## CONCLUSIONS

The series of linear monovalent alcohols provides a tool for systematically investigating specific solvent effects on photophysical properties of indicators in solution. The oligomeric nature of the molecules can further help in interpretations of related problems in polymeric matrices.

## ACKNOWLEDGMENTS

We are indebted to AVL Company and to FWF (Project No. S 5703) for funding the project and to Prof. H. Kauffmann, Vienna, for supplying the dye laser.

## REFERENCES

- 1a. A. Juris, V. Balzani, F. Barigelletti, S. Campagna, P. Belser, and A. von Zelewsky (1988) *Coord. Chem. Rev.* **84**, 85–277.
- 1b. K. Kalyanasundaram (1982) *Coord. Chem. Rev.* **46**, 159–244.
- 1c. T. J. Meyer (1986) *Pure Appl. Chem.* **58**, 1193–1206.
- 2a. N. J. Turro (1978) *Modern Molecular Photochemistry*, Benjamin/Cummings, Menlo Park, CA.
- 2b. J. V. Caspar and T. J. Meyer (1983) *J. Am. Chem. Soc.* **105**, 5583–5593.
3. B. Bagchi, D. W. Oxtoby, and G. R. Fleming (1984) *Chem. Phys.* **86**, 257–267.
4. J. Van Houten and R. J. Watts (1976) *J. Am. Chem. Soc.* **98**, 4853–4858.
5. C. A. Parker and W. T. Rees (1960) *Analyst* **85**, 587–600.
6. H. Yersin, H. Otto, J. I. Zink, and G. Gliemann (1980) *J. Am. Chem. Soc.* **102**, 951–955.
7. P. W. Atkins (1992) *Physical Chemistry*, 4th ed., Oxford Press, Oxford.
8. E. M. Kober and T. J. Meyer (1985) *Inorg. Chem.* **24**, 106–108.
9. W. J. Dressick, J. Cline III, J. N. Demas, and B. A. DeGraff (1986) *J. Am. Chem. Soc.* **108**, 7567–7574.
10. P. Hartmann, M. J. P. Leiner, S. Draxler, and M. E. Lippitsch (in preparation).
11. S. K. Garg and C. P. Smyth (1965) *J. Phys. Chem.* **69**, 1294–1301.